Control of nanoparticle formation in reactive plasmas and its application to fabrication of green energy devices

M. Shiratani

Graduate School of Information Science and Electrical Engineering, Kyushu University, Fukuoka, Japan

G. Uchida, K. Kamataki, H. Seo, N. Itagaki, K. Koga

Center of Plasma Nano-interface engineering, Kyushu University, Fukuoka, Japan

Abstract

We are developping "plasma nano-factories" which are bottom-up guided assembly processes and miniature versions of macroscopic conventional factories. Here, we report plasma-based control of the size, size distribution, and structure of nanoparticles, their agglomeration and transport as well as sticking. We apply nano-particle films to green energy devices such as low energy consumption LSI's, solar cells, and Li ion batteries. Our results show that core-shell nanoparticles are effective for improving performances of these devices.

1. Introduction

Recent developments in nanomaterials have led to new opportunities of applying them to an increasing number of applications in electronics, optoelectronics, medical components *et al* [1-11]. One of our interests has been concerned with energy conversion devices using Si nanoparticles, because the technologically important and abundant material Si is the backbone of the electronics industry. To realize the green energy devices using nanoparticles, we develop a "plasma nano-factories" which is a miniature version of macroscopic conventional fabrication, based on the knowledge of nanoparticle formation in reactive plasma [12-16]. A plasma nano-factories produces nanoblocks and radicals (adhesives) in reactive plasmas, transports nanoblocks toward a substrate and arranges them on the substrate as shown in Fig. 1 [17-22]. There are three advantages of a nano-factories in plasma: controlled agglomeration and transport of nanoblocks as well as parallel processing over large area at relatively low temperature. First, we describe fabrication of core-shell Si nanoparticle films using SiH_4/H_2 and CH_4 or N_2 double multi-hollow discharge plasma CVD. Then, we show application of Si nanoparticles to next generation solar cells and lithium ion batteries [23-25].

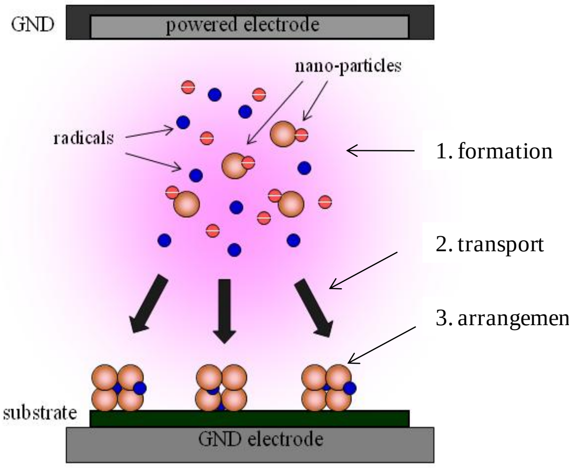

Figure 1. Concept of plasma nano-factories.

2. Deposition of core-shell nanoparticles films

Production of Si nanoparticles and surface treatment by hydrocarbon or nitrogen radicals were carried out using a multi-hollow discharge plasma CVD method as shown in Fig. 2, where two discharge plasmas of SiH_4/H_2 (plasma 1) and CH_4 or N_2 (plasma 2) were independently generated in a vacuum chamber. The multi-hollow electrode consisted of a powered electrode and two grounded electrodes of 30 mm diameter, and discharges were sustained in eight small holes of 5 mm diameter. Plasma 1 was generated by applying an rf power of 30 W to the powered electrode at SiH_4 and H_2 flow rates of 2 and 448 sccm, respectively. Si nanoparticles were nucleated, grown in SiH_4/H_2 plasma produced inside small holes, and transported downstream by a strong SiH_4/H_2 neutral gas flow. Si nanoparticles about 4 nm in average size were produced at the gas pressure of 5 Torr. The nanoparticle size can be controlled by changing pressure. Hydrocarbon or nitrogen radicals, which were produced in CH_4 and N_2 plasma at a CH_4 and N_2 flow rate of 2 and 100 sccm, respectively, were irradiated to the surface of Si nanoparticles during their transport downstream. Si nanoparticle films were deposited on substrates located downstream 67 mm from the multi-hollow electrodes, and the substrate temperature was 180°C.

Nitrogen content in Si nano-particle films was evaluated by measuring N-Ka fluorescence intensity obtained from X-ray fluorescence (XRF) measurements. As is found in Fig. 3 (a), Nitrogen content increases with approaching to the position of the N_2 discharge, whereas Si content is almost constant (see Fig. 3(b)). Double multi-hollow discharge plasma CVD method realizes combinatorial deposition of nitridated Si nano-particle films.

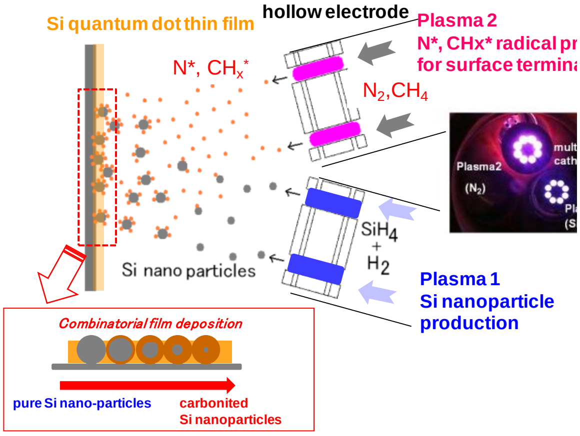

Figure 2. Schematic of experimental apparatus of double multi-hollow discharge plasma CVD.

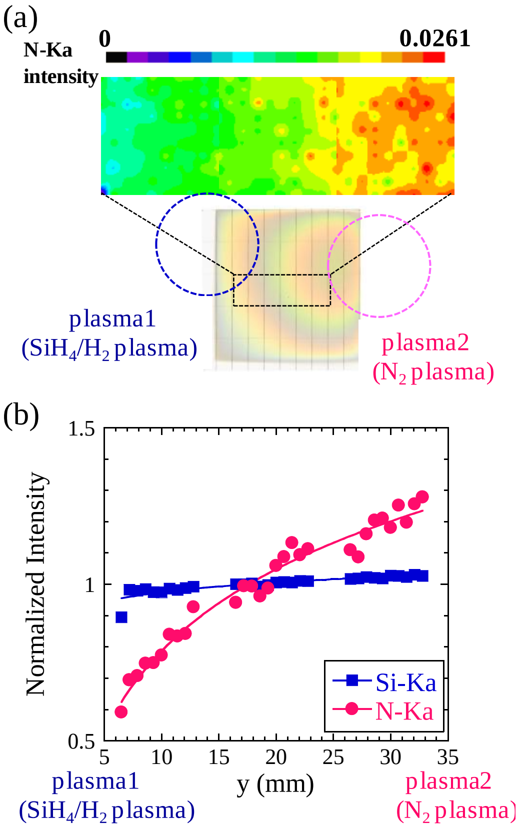

Figure 3. (a) Two-dimensional distribution of N-Kα fluorescence intensity obtained from X-ray fluorescence (XRF) measurement. (b) Substrate position dependence of N-Kα and Si-Kα fluorescence intensities from XRF.

3. Application to green devices

(1) Application to quantum-dot sensitized solar cells

SiN-Si and SiC-Si core-shell nanoparticle films were employed as sensitizers for TiO_2 photoelectrodes as shown in Fig. 4. Polysulfide electrolyte solution was used to fill the space between the TiO_2 electrode and an Au-coated FTO counterelectrode. The short-circuit current density of Si QD sensitized solar cells increases by a factor of 2.5 by irradiation of CH_4 plasma to Si nanoparticle surface. We also have measured incident photon-to-current conversion efficiency (IPCE) in the near-ultraviolet range using quartz-glass plates as front panels of QD sensitized solar cells. IPCE gradually increases by light irradiation in a wavelength range less than 600 nm around optical band-gap (E_g) of Si nanoparticle films, and then steeply increases below 280 nm around $2E_g$. This rapid increase of IPCE under short incident light may be attributed to the theoretically predicted multiple exciton generation (MEG), the creation of more than two electron-hole pairs from one high-energy photon, in nanoparticle QDs.

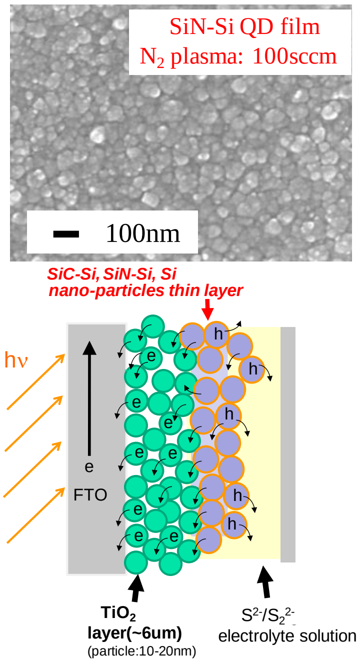

Figure 4. (a) SEM image of SiN nanoparticle films. (b) Cell structure of quantum-dot sensitized solar cells.

(2) Application to lithium ion batteries

SiC-Si core-shell nanoparticle films were used as an anode material as shown in Fig. 5, because Si has the high charge-discharge capacity up to 4200 mAh/g. The electrolyte was 1M $LiPF_6$ in ethylene carbonate (EC)/ dimethylene carbonate (DMC) (1:2). For measurements of anode properties, a Li metal sheet of 1 mm in thickness was used as a cathode. Li intercalation capacity was measured with a constant current of 0.1 mA/mg. Charge-discharge capacity of the SiC nano-composite anode of the first cycle was 3000 mAh/g, which is 9 times higher than the capacity of Li ion batteries using the conventional graphite anode.

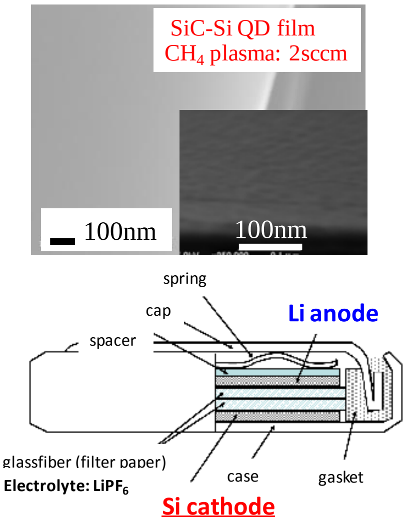

Figure 5. (a) SEM image of SiC nanoparticle films. (b) Cell structure of Li ion batteries.

4. Conclusions

We successfully developed quantum-dot sensitized solar cells and Li ion batteries using Si nanoparticles. We found that core-shell structure of Si nanoparticles is effective for improving the device performances, and observed a drastic increase in the short-circuit current density of Si QD sensitized solar, and in the charge-discharge capacity of Li ion batteries.

Acknowledges

This work was partly supported by the New Energy and Industrial Technology Development Organization (NEDO), the Ministry of Education, Culture, Sports, Science and Technology in Japan (MEXT), the Japan Society for the Promotion of Science (JSPS), Photovoltaic Power Generation Technology Research Association (PVTEC), and the Japan Science and Technology Agency (JST). We acknowledge stimulating discussions with Prof. T. Ishihara (Kyushu Univ.), Dr. M. Kondo (AIST), Dr. Y. Takeuchi (MHI), and Mr. T. Higuchi (PVTEC).

Referances

[1] D. Majumder, *et al*., IETE Tech. Rev., 24 (2007) 9.
[2] P. Rutkevych, *et al*., Phys. Plasmas, 14 (2007) 0435025.
[3] C. Joachim, *et al*., Nature, 408 (2000) 541.
[4] V. Gill, *et al.*, Int. J. Solids Structures, 45 (2008) 943
[5] I. Ennen, *et al*., J. Appl. Phys., 102 (2007) 013910.
[6] N. Khanduja, *et al*., Appl. Phys. Lett., 90 (2007) 083105.
[7] A. Nel, *et al*., Science, 311 (2006) 622.
[8] X. Wang, *et al*., Aerosol Sci. Technol., 39 (2005) 624.
[9] A. Heeren, *et al*., Microelectron. Eng., 84 (2007) 1706.
[10] J. W. G. Wildoer, *et al*., Nature, 391 (1998) 59.
[11] V. Balzani. *et al*. Nanotoday, 2 (2007) 18.
[12] M. Shiratani, *et al*., J. Phys. D: Appl. Phys., 44 (2011) 174038.
[13] K. Ostrikov, Rev. Mod. Phys., 77 (2005) 489.
[14] M. Meyyappan, *et al*., Plasma Source Sci. Technol., 12 (2003) 205
[15] T. Okada, *et al*., Chem. Phys. Lett., 417 (2006) 288.
[16] M. Mozetic, *et al*., Adv. Mater., 17 (2005) 2138.
[17] M. Shiratani, *et al*., Faraday Discuss., 137 (2008) 127.
[18] S. Iwashita, *et al*., Plasma Sources Sci. Technol., 21 (2012) 032001.
[19] K. Kamataki, *et al*., Appl. Phys. Exp., 4 (2011) 105001.
[20] K. Kamataki, *et al*., J. Inst., 7 (2012) C0417.
[21] S. Iwashita, *et al*., Jpn. J. Appl. Phys., 47 (2008) 6875.
[22] W. M. Nakamura, *et al*., Surf. Coat. Technol., 105 (2010) 5241.
[23] T. Ishihara, *et al*., Electrochem. Solid-State Lett., 10 (2007) A74.
[24] G. Uchida, *et al*., Phys. Status Solidi C, 1-4 (2011) 20100229.
[25] G. Uchida, *et al*., Jpn. J. Appl. Phys., 51 (2012) 01AD01.